



in the clean room - separates the cavity vacuum from the insulation vacuum of the cryostat and splits up the coupler mechanism from the prepared cavity. The high-purity alumina ceramics and the vacuum seal have been developed in a fruitful cooperation with FRIATEC, Mannheim.



Figure 3: Cold alumina window before (right) and after Ge plating

The ceramic surface has been coated to protect the window from static discharges and to lower the multipacting effects on the ceramic surface. For this coating, undoped amorphous Ge has been chosen because of its very low secondary emission coefficient, the stability, the thermal match and the moderate energy gap. The antistatic cover of 80 nm Ge was applied by the IKP Detector group.

Table 1: Comparison of vase-type windows of COSY and GSI Linacs and thermal data at the indicated window temperature  $T_w$

	COSY Cavity	GSI 1-gap reso.
Frequency	160 MHz	108.5 MHz
RF peak power	4 kW	160 kW
Duty factor	2%	25%
Tang. E-field	0.4 MV/m	0.2 MV/m
Acc.-gap length	35 mm	100 mm
Acc.-gap tension	0.5 MV	2.2 MV
Dimen. Feeder line	27.6mm/12mm	87.5mm/38mm
Tension at low refl.	635 V	4 kV
Diff. of pressure	0	1 atm.
Purity of alumina	99.7%	98%
Antistatic cover	Ge both sides	Li-Mo bronze
Window temp. $T_w$	10 K	370 K
Diele.-loss tangent	1E-5	0,6E-3
Diele.-loss density	some mW/cm <sup>2</sup>	110mW/cm <sup>2</sup>
Therm.conductivity	d/dt > 0	d/dt < 0
Thermal elongation	< 0.2E-6/K	6E-6/K

Dome windows were used and analysed in detail in the seventies at the GSI [4,5,6]. It turned out that the life times of the domes were shortened mainly by three factors: a) the purity of ceramics, b) imperfect surface coating and c) a high level of x-rays near 1 MeV as produced in the single-gap cavities. Table 1 compares operating conditions for the GSI and COSY windows. In

contrast to the GSI domes, our operating conditions are relaxed, especially with respect to the x-ray level from the accelerating gap and the danger of multipacting in the vicinity of the ceramics.

## CAVITY OPERATION

All measurements have been done using the RF main coupler and the tuner as designed for the COSY linac. The main coupler was tested at a pulsed RF-power up to 4 kW at a pulse length of 10 ms and a repetition rate of 2 Hz [7]. Only small changes of a spring contact were necessary to reach a routinely failure free operation at the design values. The first multipacting levels in the coupler occurred at a RF power of about 20 W and disappeared after a conditioning phase of several minutes. The variability of the coupling [8] was a great advantage during the prototype tests. This allowed precise measurements of the unloaded  $Q_0$  as well as pulsed operation at an external  $Q_{ext}$  matched to the expected beam current.

Substantial multipacting (MP) activity was found during the first cold cavity tests at low field levels. This 2-point MP is located at the beam ports and we needed about 3 weeks to overcome this barrier.

The first measurements of  $Q_0$  versus  $E_{peak}$  at an operating temperature of  $t_{bath} = 4.2$  K are presented in Figure 4. Both cavities showed very similar results. They quenched at a peak field of 31 MV/m in CW operation and at 36 MV/m in pulsed mode of 10 ms pulse width and 2 Hz repetition rate after changing the coupling strength ( $Q_{Ext}$ ) to about  $2 \cdot 10^6$ . Noticeable is the relatively high Q-slope of both cavities. The Q-values at low field levels were nearly as good as could be expected given an ambient magnetic field of 0.01 mT.

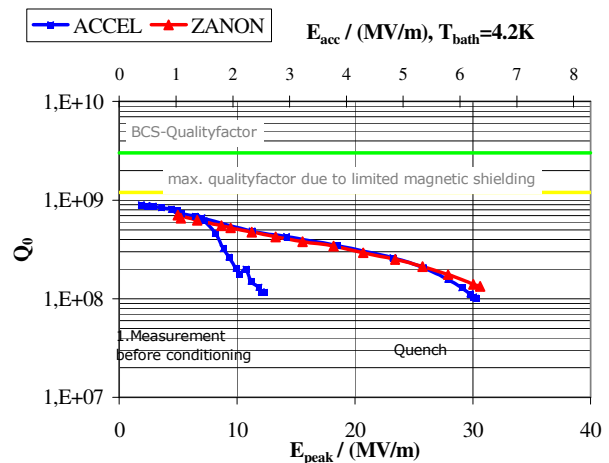


Figure 4: First measured values of  $Q_0$ - versus  $E_{acc}$ . Red: ZANON, blue: ACCEL

The ACCEL prototype showed additional multipacting levels starting at  $E_{acc} = 1$  MV/m. These weak MP barriers had been easily conditioned within some minutes. Field emission starts at an accelerating field-level of about 4.5 MV/m at both cavities.

### Pulsed operation

Both cavities have been operated in pulsed mode. The RF coupler has been moved to reach an external Q-value of about  $4 \cdot 10^6$  which is nearly the optimum Q-value to accelerate a beam of 2 mA. The Lorentz-force detuning was measured in pulsed mode to reduce the influence of the He-bath pressure. The lengths of the pulses were long enough to reach the steady state. Fig. 5 shows the measured Lorentz-force detunings (LFD) and the linear approximations. The resulting Lorentz-force constants of  $6 \text{ Hz} / (\text{MV/m})^2$  (ZANON) and about  $10 \text{ Hz} / (\text{MV/m})^2$  (ACCEL) are significantly higher compared to the simulations where a Lorentz-force constant of  $1 \text{ Hz} / (\text{MV/m})^2$  was predicted [9].

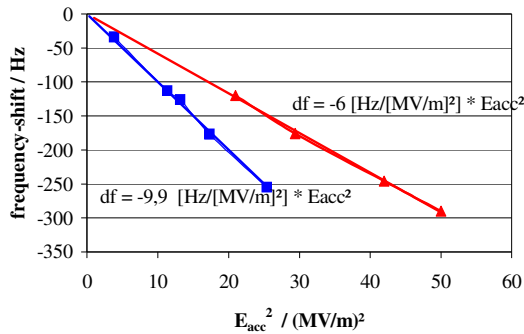


Figure 5: Measured Lorentz-force detuning

The actuating mechanics of the tuner for each HWR consists of two parts: a stepper motor driving the coarse tuner and a piezo fine tuner, both mounted outside the cryostat. The possible change of the lengths of the high-voltage piezos is about  $+120 \mu\text{m}$ . A gear of 1:6 minimizes the microphonic effects of the long tuning rods and lowers the tuning forces but reduces the corresponding tuning range of the cavity.

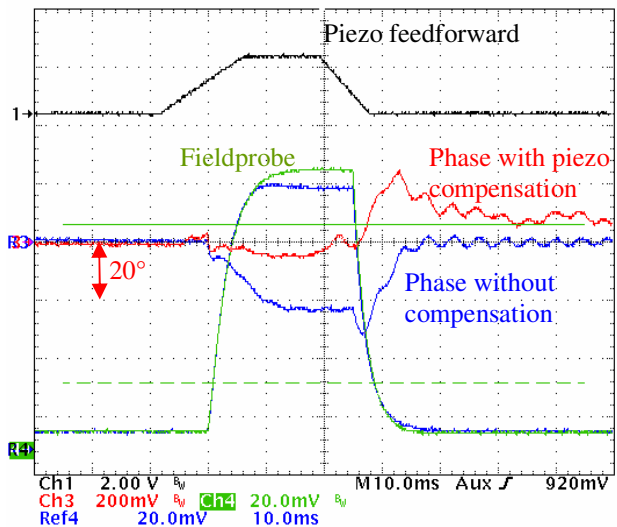


Figure 6: Compensation of LFD at an accelerating field of  $E_{\text{acc}}=3.1 \text{ MV/m}$  (ZANON cavity) with fast piezo tuning-system

The resulting strain of the cavity is sufficient to compensate for the Lorentz-force detuning during the pulsed operation with the fast piezo tuner [10]. The detuning itself stays within the operating range of the fast piezo-system, but the large rising time in combination with the high voltage at the piezos required for an overall compensation of the LFD limits the use of the piezos.

So far the tuner itself is not backlash free; this can be included in the feedforward curve of the piezos but generates additional limitations. Figure 6 presents the first results of LFD compensation tests in a generator-driven mode. The change of the resonant frequency at the moderate field-level of  $3.1 \text{ MV/m}$  corresponds nearly to the LFD at the desired accelerating field of  $8 \text{ MV/m}$  expected by the computer simulation. Comparing the phase shifts with and without compensation demonstrates a reduction of the phase error of about 90%. The phase was measured between the field probe and the RF-generator.

### Mechanical resonances

Mechanical resonances play an important role in the pulsed operation of a superconducting cavity. Two methods have been employed to find all significant resonances. One measurement of the mechanical eigenmodes is presented in Figure 7. The excitation of the mechanical resonances by a step function from the piezo tuner can be classified after taking the fast Fourier transform of the phase signal within a phase locked loop operation.

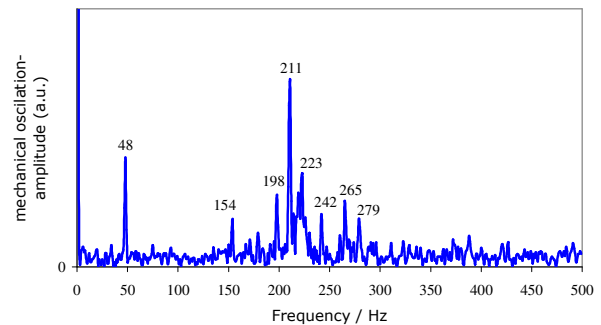


Figure 7: Fast Fourier Transformation of phase-detector signal (ACCEL cavity) responding to a 50 V step function from the piezos.

The first mechanical resonance frequency (48 Hz) is rather low and near 50 Hz, but nevertheless it doesn't influence the normal cavity operation. The behaviour of the cavity in the pulsed mode is dominated by the strongest resonance at 211 Hz. Fig. 8 illustrates the onset of this eigenmode only by RF pulses and a strong coupling. This oscillation prevents an undisturbed operation of the frequency-control loop. All resonances were found in the ZANON cavity, as well, except that all the frequencies are higher by 10%. The smaller Lorentz-force constant and the higher resonances are the consequence of the stronger end-plates and the additional stiffening by the higher number of weldings. Nevertheless

routine operations in pulsed mode require even better mechanical stability for both cavities.

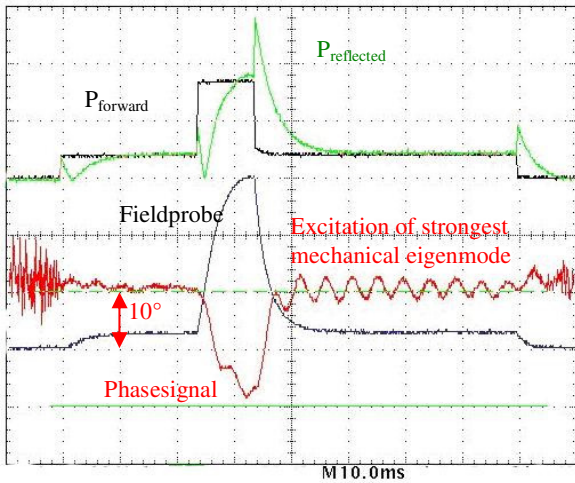


Figure 8: Similar to Fig. 6, but the generator frequency is locked to the RF eigenfrequency of the cavity and LFD compensation is not applied (ACCEL cavity)

*I/Q Field control*

In Fig. 9 the simplified RF-system for the prototype tests is shown. The attenuator Att3 is configurable and will be used in a feedforward for compensation of the

effects of beam loading. The attenuators Att1 and Att2 belong to the designed pulse circuit and allow a quasi-stable phase regulation for power pulses of different heights and widths. The use of a transistor-based power amplifier makes a pulse scheme according Figure 10 possible. A small RF field is maintained in the cavity all the time. The frequency control of the cavity is performed between the pulses at the RF socket. The high resolution of the stepper motor system of about 1.2 Hz per step allows a frequency control based only on this stepper motor, corresponding to a frequency-change rate of 2.4 kHz/s. The tuning sensitivity of 120 kHz/mm is large enough to compensate for fabrication tolerances.

A gate circuit holds the resonance frequency within a range of +/- 15 Hz. The trigger-point TP1 activates the fast analogue I/Q control and disables the stepper-motor of the frequency-control loop. At TP2 the forward power is increased to reach the nominal accelerating field, while the fieldprobe signal to the I/Q control circuit is decreased to maintain the operating point of the steady-state case. TP3 disables the I/Q control and switches the RF-power back to the value of the CW socket. The analogue I/Q control circuit is mainly based on a proportional and integral term adapted to the specific developed I/Q modulator and the commercial I/Q demodulator. Its bandwidth has a value of around 5 MHz.

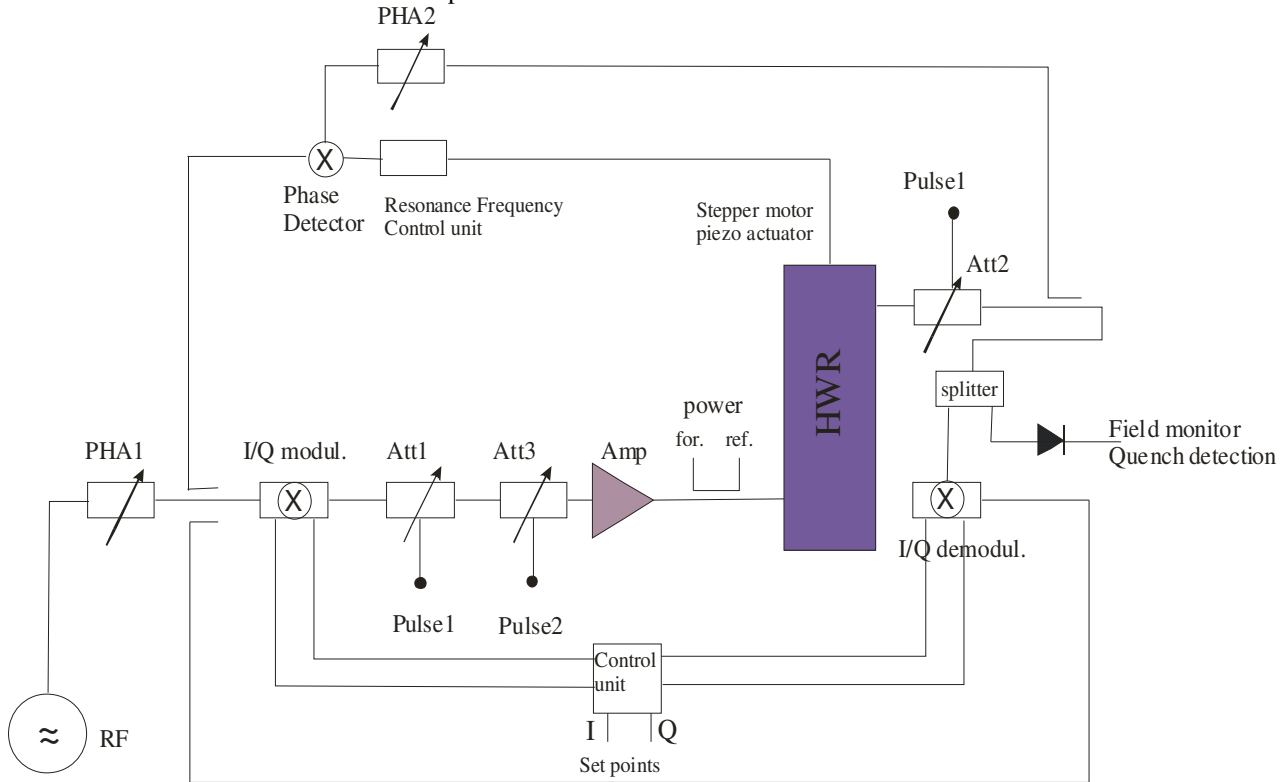


Figure 9: Block diagram of the HWR control: PHA1, PHA2 programmable phase shifters, ATT1, ATT2, ATT3 programmable attenuators; pulse1 = TP2 and TP3 in Fig. 10, pulse2 = beam-feedforward pulse

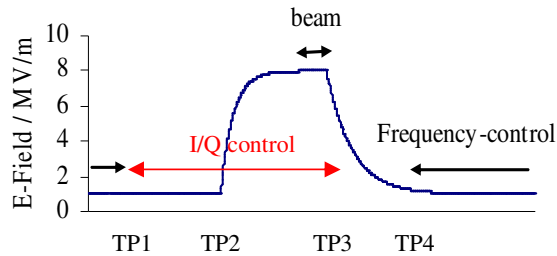


Figure 10: Trigger points, accelerating field levels of RF pulse and CW socket

Figure 11 shows the behaviour of the I/Q control circuit at the bounds of the stepper-motor control loop of  $\pm 14$  Hz. Larger deviations of the resonant frequency will be compensated by the frequency control loop during the pulse pauses. Thus Fig. 11 represents the worst case of the I/Q control. During the first test run we reached an amplitude accuracy of  $\pm 0.6\%$  and  $\pm 1.4^\circ$  in phase, which is already close to the design values of  $\pm 0.5\%$  in amplitude and  $\pm 0.5^\circ$  in phase. The residual accuracy within the pulse is about a factor of 6 better. An increase of the amplitude and phase accuracy of the I/Q control loop can easily be reached by reducing the window of the frequency control loop after minimizing the dominant mechanical eigenmode.

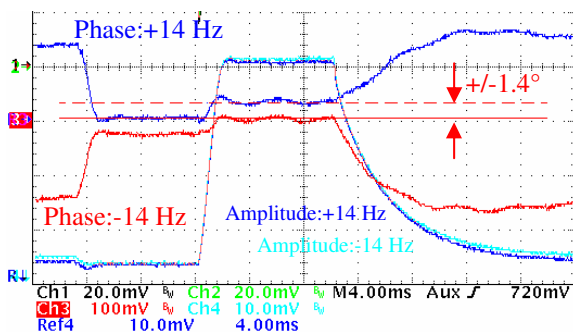


Figure 11: Phase and amplitude accuracy of the I/Q control loop regarding the worst case

## OUTLOOK

The results obtained from the first prototype cavity are very promising. The design gradient of 6 MV/m (goal 1) has been exceeded during the first tests. Achieving the even more demanding goal 2 (8 MV/m in pulsed operation) seems to be within reach. Therefore, long-term RF conditioning and baking will also be performed. A prototype of the cryostat is under fabrication and will be completed and tested at the end of this year [11]. One prototype cavity will be completed with a titanium LHe cover and installed in the new cryostat. This configuration will allow an operational test of a COSY linac cryostat without beam.

## ACKNOWLEDGMENT

We acknowledge the support of the European Community-Research Infrastructure Activity under the FP6 "Structuring the European Research Area" program (CARE, contract number RII3-CT-2003-506395).

## REFERENCES

- [1] R. Maier, U. Bechstedt, N. Bongers, J. Dietrich, O. Felden, R. Gebel, K. Henn, H. Jungwirth, A. Lehrach, N. Markgraf, U. Pfister, D. Prasuhn, P. von Rossen, A. Schempp, A. Schnase, H. Schneider, Y. Senichev, R. Stassen, H. Stockhorst, R. Toelle, E. Zaplatin, The superconducting injector linac for the Cooler-Synchrotron COSY at FZ-Juelich, Proc. LINAC2002, Korea, 2002.
- [2] R. Toelle, U. Bechstedt, N. Bongers, J. Dietrich, A. Facco, O. Felden, R. Gebel, K. Henn, H. Jungwirth, A. Lehrach, R. Maier, N. Markgraf, U. Pfister, D. Prasuhn, P. von Rossen, A. Schempp, A. Schnase, H. Schneider, Y. Senichev, R. Stassen, H. Stockhorst, E. Zaplatin, V. Zviagintsev, A Superconducting Injector Linac for COSY, Proc. EPAC2002, Paris, 2002.
- [3] R. Eichhorn, F.M. Esser, B. Laatsch, G. Schug, H. Singer, R. Stassen, E. Zaplatin, Development of a pulsed Light Ion Accelerator Module based on Half-Wave Resonators, Proc. SRF2003, Luebeck, 2003.
- [4] U. Grundinger, Hochfrequenz-Einspeisung in den 108MHz-Einzelresonator, UNILAC-Projektbericht 1, GSI 74-1, Sept.71, S.15...16
- [5] D. Böhne, M. Emmerling, A. Gasper, Recent improvements of accelerator components at the UNILAC, Lin.Ac. Conf. 1979
- [6] D. Böhne, W. Karger, E. Miersch, W. Röske, B. Stadler, Sparking measurements in a single-gap cavity, Part. Acc. Conf. 1971, IEEE Trans. NS-18, 568...571
- [7] R. Stassen, R. Eichhorn, F.M. Esser, B. Laatsch, R. Maier, G. Schug, R. Toelle, First results of pulsed superconducting Half-Wave-Resonators, Proc. EPAC2004, Luzern, Switzerland, 2004.
- [8] G. Schug, H. Singer, R. Stassen, The adjustable RF main coupler for the superconducting COSY Linac cavities, FZJ/IKP Annual Report 2002, Juelich, 2002
- [9] E. Zaplatin, private communication
- [10] M. Liepe, W.D. Moeller, S.N. Simrock, Dynamic Lorentz Force Compensation with a Fast Piezoelectric Tuner, PAC 2001, Chicago, USA, 2001, p.1074
- [11] R. Eichhorn, F. Esser, B. Laatsch, M. Lennartz, G. Schug, R. Stassen, Results of the Juelich accelerator module based on superconducting half-wave resonators, Cryogenic Engineering Conference, to be published